

Load frequency control for multi-area power system with two-source using sliding mode control

Quoc Thai Phan¹, Thanh Lam-The Tran¹, Phat Tuan Le¹, Dinh Bao Ho¹, Van Van Huynh²

¹Faculty of Electrical and Electronics Engineering, Ton Duc Thang University, Ho Chi Minh City, Viet Nam

²Modeling Evolutionary Algorithms Simulation and Artificial Intelligence, Faculty of Electrical and Electronics Engineering, Ton Duc Thang University, Ho Chi Minh City, Viet Nam

Article Info

Article history:

Received Sep 9, 2024

Revised Apr 7, 2025

Accepted Jul 2, 2025

Keywords:

Integral sliding surface

Load frequency control

Power system control

Sliding mode control

Three-area interconnected power system

ABSTRACT

A consistent electrical supply relies on the stability of power systems. In changing load conditions, control methods like load frequency control (LFC) are essential for safeguarding its stability. Conventional methods of LFC frequently encounter uncertainties in the system, external disruptions, and nonlinearities. This article introduces a more sophisticated method for managing load frequency and improving LFC in power systems through the utilization of sliding mode control (SMC). SMC provides strong stability and resilience against nonlinearities and disturbances, making it a promising method to overcome the drawbacks of traditional control techniques. We offer an in-depth examination of the second-order-integral SMC (SOISM) method specifically designed for LFC, covering the creation and execution of the control algorithm. The method being suggested utilizes a sliding/gliding surface to maintain the system trajectories as continuous on the surface even with changes in parameters and external disturbances. Simulation results show big enhancements in frequency stability and system performance when compared to conventional proportional-integral-derivative (PID) controllers. The article also features a comparison between SOISM and other contemporary control methods, emphasizing its strength in terms of resilience and flexibility.

This is an open access article under the [CC BY-SA](https://creativecommons.org/licenses/by-sa/4.0/) license.



Corresponding Author:

Van Van Huynh

Modeling Evolutionary Algorithms Simulation and Artificial Intelligence

Faculty of Electrical and Electronics Engineering, Ton Duc Thang University

19 Nguyen Huu Tho Str., Tan Phong ward, District 7, Ho Chi Minh City, Vietnam

Email: huynhvanvan@tdtu.edu.vn

1. INTRODUCTION

Due to the growing process of industrialization and modernization, the demand for electrical energy is constantly increasing. This poses challenges to maintaining stable frequencies in multi-source, multi-area power interconnected systems (MSMAIPS) with frequent generation and load variations fluctuations. Frequency instability can affect the power system's (PS) operation and reliability. Large frequency deviations can affect the lifespan of equipment, causing system imbalance or overloading the transmission line, affecting the protection ability of the system, and eventually leading to damage to electrical equipment. To solve these load frequency control problems (LFCP), load frequency control (LFC) has been applied.

Various approaches of classical proportional (P), proportional-integral (PI), and proportional-integral-derivative (PID) have been made throughout recent years. A Laurent series-based PID controller controls single and multi-area PS in [1]. A fuzzy PI/PID controller is used with integration of differential evolution and pattern search for optimized gains in [2]. A second-order neural network is also employed to tackle

LFCP in multi-microgrid PS [3]. Cascaded controllers such as fractional-order-PI and fractional-order-PD are proposed to control a hydro-thermal PS in [4]. A PID controller is compared by using an adaptive fuzzy logic controller with H_∞ criterion in [5]. These approaches improve the reactivity and optimize the controllers in order to reduce and converge the area control error with frequency deviation to zero as fast as possible.

The model predictive control (MPC) approach is also widely used for LFCP. An MPC controls MS-MAIPS with consideration of generate rate constraints (GRC) in [6]. Another approach uses disturbance rejection for MSMAIPS in [7]. Furthermore, in [8], an MPC is also used for PS with renewable energy - wind energy. By advancing MPC, adaptive MPC with Kalman filter is used for high-penetration renewable energy microgrids in [9]. An LMI-delay margin estimation-based controller for PS with communication delay is presented in [10]. An event-triggered-based controller is used for PS with time delay in [11]. These researches provide deep understanding of various control methods on many PS scenarios.

The sliding mode control (SMC) approach greatly increases the robustness of control in LFCP. Therefore, in recent years, SMC has been used in various research on LFCP. Many applications of SMC are introduced in [12]. The chattering problem of SMC is rejected due to the successful implementation of second-order SMC in [13]. A second-order SMC with the extended observer is used for robust LFC in [14]. Furthermore, third-order SMC with state observer is developed in [15]. SMC is also used for PS with the cooperation of wind power and time-delay consideration in [16]. Research in [17] does the same thing but tops it off with droop and pitch angle control then proceeds to test it using the IEEE 39 bus system. Another second-order SMC with adaptive behavior and communication-delay PS is investigated in [18]. Battery energy storage system (BESS) is also used with SMC in [19]. Classical SMC is further optimized by smart algorithms such as grey wolf optimization (GWO) and particle swarm optimization (PSO) in [20]. Adaptive high-order SMC is also applied in [21]. Linear matrix inequality (LMI) approach for the dynamic integral SMC with consideration of time delay is researched in [22]. Backstepping-based SMC is proposed in [23] and compared with other advanced SMCs. Electrical vehicle aggregators are considered for LFCP in [24] and modified PSO-based Integral SMC is used. A H_∞ state feedback for SMC with delayed communication is developed in [25]. These SMC controllers deal with many types of LFC problems and the SMC controller problem itself, promoting high stability of the PS.

This paper provides a thorough research of the latest improvements in SMC for LFCP, with a concentration on MSMAIPS. With the integration of many recent highly innovative pieces of research, we aim to achieve a controller that can adapt to many PS and fix the SMC chattering problems for optimized LFC behavior.

2. MATHEMATICAL MODEL OF TWO-SOURCE, MULTI-AREA POWER SYSTEM

The examined system is a two-source, multi-area power system (TSMAPS) consisting of two generation sources in each area and a total of three areas. Figure 1 represents all the components of the TSMAPS. The subsections show the mathematical state-space expressions of all areas.

2.1. Area 1's system model

A control area within a power system often integrates both thermal (with a non-reheat turbine) and hydro generating units, each with distinct dynamic characteristics. While the thermal unit provides a simplified dynamic response, the hydropower plant offers rapid response capabilities essential for absorbing sudden load changes. Area 1's dynamic equations are derived below.

$$\Delta P_{tie,1} = \Delta P_{tie,12} - \Delta P_{tie,31} \quad (1)$$

$$\Delta \dot{f}_1 = -\frac{1}{T_{P1}} \Delta f_1 + \frac{K_{P1}}{T_{P1}} \Delta P_{m1} + \frac{K_{P1}}{T_{P1}} \Delta P_{m2} - \frac{K_{P1}}{T_{P1}} \Delta P_{tie,1} - \frac{K_{P1}}{T_{P1}} \Delta P_{L1} \quad (2)$$

$$\Delta \dot{P}_{m1} = -\frac{1}{T_{T1}} \Delta P_{m1} + \frac{1}{T_{T1}} \Delta P_{g1} \quad (3)$$

$$\Delta \dot{P}_{g1} = -\frac{1}{T_{G1}} \Delta P_{g1} - \frac{1}{T_{G1}} \Delta P_{C1} - \frac{1}{R_1 T_{G1}} \Delta f_1 \quad (4)$$

$$\Delta \dot{P}_{m2} = -\frac{2}{T_{W1}} \Delta P_{m2} + \frac{2}{T_{W1}} \Delta P_{v2} - 2 \Delta \dot{P}_{v2} \quad (5)$$

$$\Delta \dot{P}_{v2} = -\frac{1}{T_{H1}} \Delta P_{v2} + \frac{1}{T_{H1}} \Delta P_{g2} + \frac{T_{R1}}{T_{H1}} \Delta \dot{P}_{g2} \quad (6)$$

$$\Delta \dot{P}_{g2} = -\frac{1}{T_{G2}} \Delta P_{g2} - \frac{1}{T_{G2}} \Delta P_{C1} - \frac{1}{R_2 T_{G2}} \Delta f_1 \quad (7)$$

$$A \dot{C} E_1 = \Delta P_{tie,1} + B_1 \Delta f_1 \quad (8)$$

$$\Delta \dot{P}_{tie,1} = \Delta \dot{P}_{tie,12} - \Delta \dot{P}_{tie,31} = 2\pi(T_{12} + T_{31})\Delta f_1 - 2\pi T_{12}\Delta f_2 - 2\pi T_{31}\Delta f_3 \quad (9)$$

$$\Delta \dot{P}_{v2} = -\frac{1}{T_{H1}} \Delta P_{v2} + \left(\frac{1}{T_{H1}} - \frac{T_{R1}}{T_{H1}T_{G2}}\right) \Delta P_{g2} - \frac{T_{R1}}{T_{H1}T_{G2}} \Delta P_{C1} - \frac{T_{R1}}{R_2 T_{H1}T_{G2}} \Delta f_1 \quad (10)$$

$$\Delta \dot{P}_{m2} = -\frac{1}{T_{W1}} \Delta P_{m2} + \left(\frac{2}{T_{W1}} + \frac{2}{T_{H1}}\right) \Delta P_{v2} + \left(\frac{2T_{R1}}{T_{H1}T_{G2}} - \frac{2}{T_{H1}}\right) \Delta P_{g2} + \frac{2T_{R1}}{T_{H1}T_{G2}} \Delta P_{C1} + \frac{2T_{R1}}{R_2 T_{H1}T_{G2}} \Delta f_1 \quad (11)$$

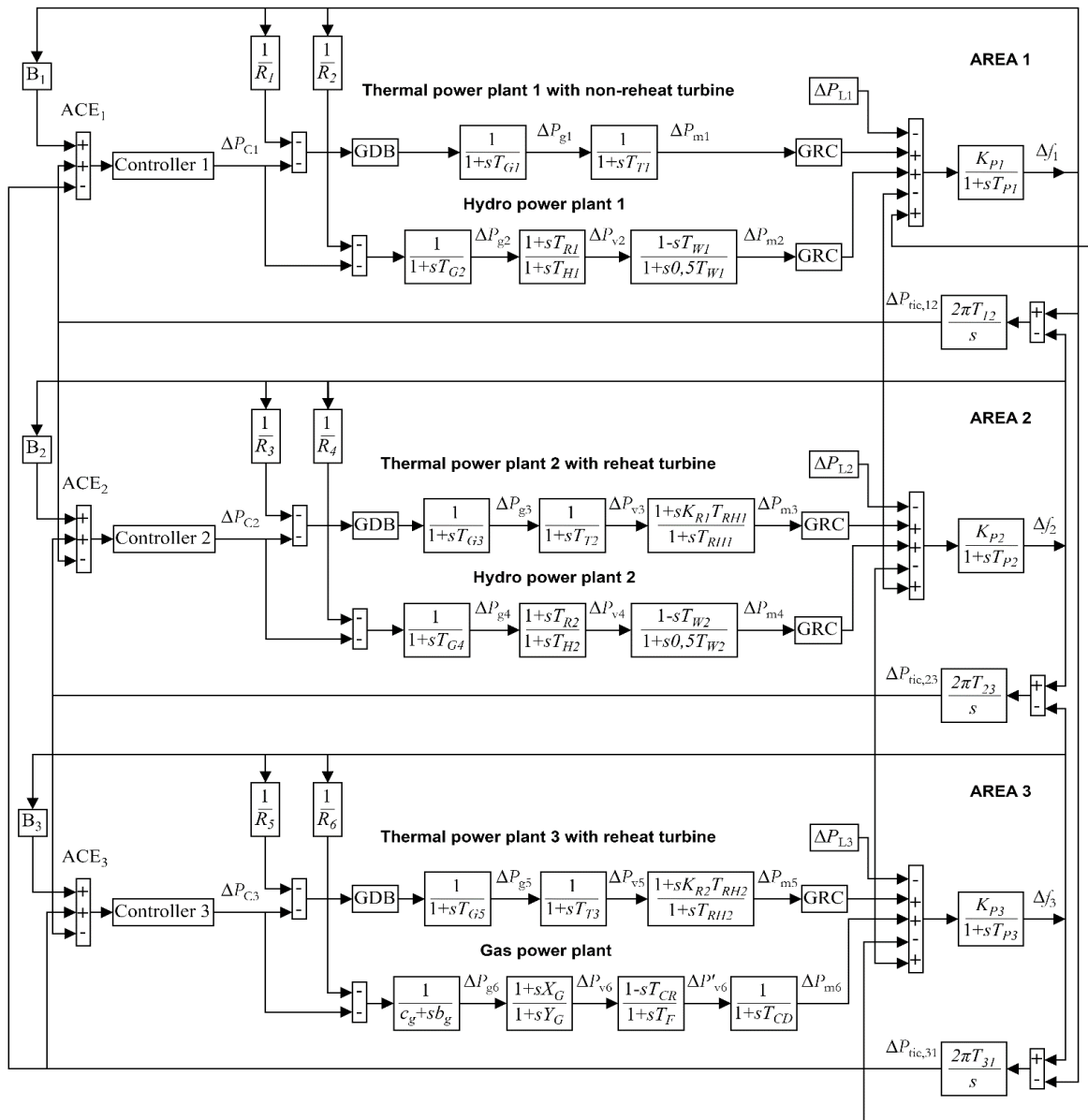


Figure 1. State-space model of the TSMAPS power system

2.2. Area 2's system model

The reheat thermal unit is an efficient base-load generator, but its reheat stage introduces a slower, more complex dynamic response than a non-reheat turbine. Integrating this slow-responding plant with a

fast-acting hydro plant demands a sophisticated and robust LFC strategy to harmonize their contrasting dynamics. The dynamic equations are also derived below.

$$\Delta P_{tie,2} = \Delta P_{tie,23} - \Delta P_{tie,12} \quad (12)$$

$$\Delta \dot{P}_{m3} = -\frac{1}{T_{RH1}} \Delta P_{m3} + \frac{1}{T_{RH1}} \Delta P_{v3} + K_{R1} \Delta \dot{P}_{v3} \quad (13)$$

$$\Delta \dot{f}_2 = -\frac{1}{T_{P2}} \Delta f_2 + \frac{K_{P2}}{T_{P2}} \Delta P_{m3} + \frac{K_{P2}}{T_{P2}} \Delta P_{m4} - \frac{K_{P2}}{T_{P2}} \Delta P_{tie,2} - \frac{K_{P2}}{T_{P2}} \Delta P_{L2} \quad (14)$$

$$\Delta \dot{P}_{v3} = -\frac{1}{T_{T2}} \Delta P_{v3} + \frac{1}{T_{T2}} \Delta P_{g3} \quad (15)$$

$$\Delta \dot{P}_{g3} = -\frac{1}{T_{G3}} \Delta P_{g3} - \frac{1}{T_{G3}} \Delta P_{C2} - \frac{1}{R_3 T_{G3}} \Delta f_2 \quad (16)$$

$$\Delta \dot{P}_{m4} = -\frac{2}{T_{W2}} \Delta P_{m4} + \frac{2}{T_{W2}} \Delta P_{v4} - 2 \Delta \dot{P}_{v4} \quad (17)$$

$$\Delta \dot{P}_{v4} = -\frac{1}{T_{H2}} \Delta P_{v4} + \frac{1}{T_{H2}} \Delta P_{g4} + \frac{T_{R2}}{T_{H2}} \Delta \dot{P}_{g4} \quad (18)$$

$$\Delta \dot{P}_{g4} = -\frac{1}{T_{G4}} \Delta P_{g4} - \frac{1}{T_{G4}} \Delta P_{C2} - \frac{1}{R_4 T_{G4}} \Delta f_2 \quad (19)$$

$$\Delta \dot{P}_{m3} = -\frac{1}{T_{RH1}} \Delta P_{m3} + \left(\frac{1}{T_{RH1}} - \frac{K_{R1}}{T_{T2}} \right) \Delta P_{v3} + \frac{K_{R1}}{T_{T2}} \Delta P_{g3} \quad (20)$$

$$\Delta \dot{P}_{v4} = -\frac{1}{T_{H2}} \Delta P_{v4} + \left(\frac{1}{T_{H2}} - \frac{T_{R2}}{T_{H2} T_{G4}} \right) \Delta P_{g4} - \frac{T_{R2}}{T_{H2} T_{G4}} \Delta P_{C2} - \frac{T_{R2}}{R_4 T_{H2} T_{G4}} \Delta f_2 \quad (21)$$

$$\Delta \dot{P}_{m4} = -\frac{2}{T_{W2}} \Delta P_{m4} + \left(\frac{2}{T_{W2}} + \frac{2}{T_{H2}} \right) \Delta P_{v4} + \frac{2 T_{R2}}{T_{H2} T_{G4}} \Delta P_{C2} + \left(\frac{2 T_{R2}}{T_{H2} T_{G4}} - \frac{2}{T_{H2}} \right) \Delta P_{g4} + \frac{2 T_{R2}}{T_{H2} T_{G4} R_4} \Delta f_2 \quad (22)$$

$$\Delta P_{tie,3} = \Delta P_{tie,31} - \Delta P_{tie,23} \quad (23)$$

2.3. Area 3's system model

The gas power plant's rapid-response capability, due to its fast-acting turbine dynamics, makes it an invaluable resource for managing sudden load fluctuation. However, this dynamic integration introduces a new layer of complexity that must be rigorously addressed to ensure controller stability. The equations of this area's dynamic are derived below.

$$\Delta \dot{f}_3 = -\frac{1}{T_{P3}} \Delta f_3 + \frac{K_{P3}}{T_{P3}} \Delta P_{m5} + \frac{K_{P3}}{T_{P3}} \Delta P_{m6} - \frac{K_{P3}}{T_{P3}} \Delta P_{tie,3} - \frac{K_{P3}}{T_{P3}} \Delta P_{L3} \quad (24)$$

$$\Delta \dot{P}_{m5} = -\frac{1}{T_{RH2}} \Delta P_{m5} + \frac{1}{T_{RH2}} \Delta P_{v5} + K_{R2} \Delta \dot{P}_{v5} \quad (25)$$

$$\Delta \dot{P}_{v5} = -\frac{1}{T_{T3}} \Delta P_{v5} + \frac{1}{T_{T3}} \Delta P_{g5} \quad (26)$$

$$\Delta \dot{P}_{g5} = -\frac{1}{T_{G5}} \Delta P_{g5} - \frac{1}{T_{G5}} \Delta P_{C3} - \frac{1}{R_5 T_{G5}} \Delta f_3 \quad (27)$$

$$\Delta \dot{P}_{m6} = -\frac{1}{T_{CD}} \Delta P_{m6} + \frac{1}{T_{CD}} \Delta P'_{v6} \quad (28)$$

$$\Delta \dot{P}'_{v6} = -\frac{1}{T_F} \Delta P'_{v6} + \frac{1}{T_F} \Delta P_{v6} - \frac{T_{CR}}{T_F} \Delta \dot{P}_{v6} \quad (29)$$

$$\Delta \dot{P}_{v6} = -\frac{1}{Y_G} \Delta P_{v6} + \frac{1}{Y_G} \Delta P_{g6} + \frac{X_G}{Y_G} \Delta \dot{P}_{g6} \quad (30)$$

$$\Delta \dot{P}_{g6} = -\frac{c_g}{b_g} \Delta P_{g6} - \frac{1}{b_g} \Delta P_{C3} - \frac{1}{R_6 b_g} \Delta f_3 \quad (31)$$

$$\Delta \dot{C}E_3 = \Delta P_{tie,3} + B_3 \Delta f_3 \quad (32)$$

$$\Delta \dot{P}_{tie,3} = \Delta \dot{P}_{tie,31} - \Delta \dot{P}_{tie,23} = 2\pi(T_{31} + T_{23})\Delta f_3 - 2\pi T_{31}\Delta f_1 - 2\pi T_{23}\Delta f_2 \quad (33)$$

$$\Delta \dot{P}_{m5} = -\frac{1}{T_{RH2}} \Delta P_{m5} + \left(\frac{1}{T_{RH2}} - \frac{K_{R2}}{T_{T3}}\right) \Delta P_{v5} + \frac{K_{R2}}{T_{T3}} \Delta P_{g5} \quad (34)$$

$$\Delta \dot{P}_{v6} = -\frac{1}{Y_G} \Delta P_{v6} + \left(\frac{1}{Y_G} - \frac{X_G c_g}{Y_G b_g}\right) \Delta P_{g6} - \frac{X_G}{Y_G b_g} \Delta P_{C3} - \frac{X_G}{R_G Y_G b_g} \Delta f_3 \quad (35)$$

$$\begin{aligned} \Delta \dot{P}'_{v6} = & -\frac{1}{T_F} \Delta P'_{v6} + \left(\frac{1}{T_F} + \frac{T_{CR}}{T_F Y_G}\right) \Delta P_{v6} + \left(\frac{T_{CR} X_G c_g}{T_F Y_G b_g} - \frac{T_{CR}}{T_F Y_G}\right) \Delta P_{g6} + \frac{T_{CR} X_G}{T_F Y_G b_g} \Delta P_{C3} \\ & + \frac{T_{CR} X_G}{R_6 T_F Y_G b_g} \frac{T_{CR} X_G}{T_F Y_G b_g} \frac{T_{CR} X_G}{T_F Y_G b_g} \frac{T_{CR} X_G}{T_F Y_G b_g} \Delta f_3 \end{aligned} \quad (36)$$

3. OBSERVER DESIGN

A state observer is a control mechanism that delivers an approximation of the numerical internal states of a specific real system, TSMAPS in this scenario, by utilizing measurements taken from both the input and output of that system. First, state-space expression of the system is expressed as:

$$\begin{cases} \dot{\chi}_i(t) = A_i \chi_i(t) + B_i u_i(t) + \sum_{j=1}^N H_{ij} \chi_j(t) + F_i \Delta P_{Li} \\ y_i(t) = C_i \chi_i(t) \end{cases} \quad (37)$$

with, χ_i is a state vector with p state variables. Matrices A_i with dimensions of p×p. u_i is a control vector with m control variables. Matrices B_i with dimensions of p×m. χ_j is a state vector connecting to another area. Matrices H_{ij} with dimensions equal to the state variable χ_i . ΔP_{Li} is a load disturbance vector with g load disturbance variables. Matrices F_i with dimensions of p×g. y_i is an output vector with h output variables. Matrices C_i with dimensions of h×p.

Then, state-space expression of the observer is expressed as:

$$\begin{cases} \dot{\hat{\chi}}_i(t) = A_i \hat{\chi}_i(t) + B_i u_i(t) + \sum_{j=1}^N H_{ij} \hat{\chi}_j(t) + L_i [y_i(t) - \hat{y}_i(t)] \\ \hat{y}_i(t) = C_i \hat{\chi}_i(t) \end{cases} \quad (38)$$

With, $\hat{\chi}_i(t)$ is the estimated state of $\chi_i(t)$. $\hat{y}_i(t)$ is the estimated state output of $y_i(t)$. L_i is the observer gain.

4. INTEGRAL SMC

Integral sliding mode control (ISMC) with a state estimator is a robust control method to enhance the stability and performance of PS. First step is to determine the integral sliding surface (ISS). The next step is the construction of an equivalent control law and a switching law. Finally, stability analysis of the control signal. The ISS with estimated state is given as:

$$\sigma_i[\hat{\chi}_i(t)] = G_i \hat{\chi}_i(t) - \int_0^t G_i (A_i - B_i K_i) \hat{\chi}_i(\tau) d\tau \quad (39)$$

With, matrices G_i is chosen accordingly to ensure that the matrix $G_i B_i$ is nonsingular or invertible. Therefore, matrix G_i can be chosen as $G_i = B_i^{-1}$.

The general control signal is given (40).

$$u_i(t) = u_i^{eq}(t) + u_i^{sw}(t) \quad (40)$$

With, $u_i^{eq}(t)$ is the equivalent control equation (ECE) to ensure that the system is in the sliding surface and $u_i^{sw}(t)$ is the switching control equation that ensures the system will heads towards and remains on the sliding surface.

From (39) when $\sigma_i(t) = \dot{\sigma}_i(t) = 0$, the ECE becomes:

$$u_i^{eq}(t) = -(G_i B_i)^{-1} \left[G_i \sum_{j=1}^N H_{ij} \hat{x}_j(t) + G_i L_i [y_i(t) - \hat{y}_i(t)] + G_i B_i K_i \hat{x}_i(t) \right] \quad (41)$$

The switching control occurs when:

$$u_i^{sw}(t) = -\alpha_i \text{sat}[\sigma_i[\hat{x}_i(t)]] \quad (42)$$

α_i : positive constant ($\alpha_i > 0$). This factor helps to adjust the convergence speed of the system. The saturation condition that helps reduce chattering effect is given (43).

$$\text{sat}[\sigma_i[\hat{x}_i(t)]] = \begin{cases} -1 & \text{if } \sigma_i[\hat{x}_i(t)] < (-1) \\ \sigma_i[\hat{x}_i(t)] & \text{if } (-1) < \sigma_i[\hat{x}_i(t)] < 1 \\ 1 & \text{if } \sigma_i[\hat{x}_i(t)] > 1 \end{cases} \quad (43)$$

Substitute (43) and (44) into (42), we will have the general control signal is given below:

$$u_i(t) = -(G_i B_i)^{-1} \left[G_i \sum_{j=1}^N H_{ij} \hat{x}_j(t) + G_i L_i [y_i(t) - \hat{y}_i(t)] + G_i B_i K_i \hat{x}_i(t) + \alpha_i \text{sat}(\sigma_i[\hat{x}_i(t)]) \right] \quad (44)$$

Using (44) we will have $\sigma_i(t)\dot{\sigma}_i(t) < 0$. This condition will ensure that the value of $\sigma_i(t)$ will decrease over time, thereby ensuring that the sliding motion will be asymptotically stable over time.

5. SIMULATION RESULTS AND DISCUSSION

The simulation will provide the proposed controllers' response with a comparison of other controllers such as PID and ISMC. Areas of PS model are introduced to a load disturbance of follows: $\Delta P_{L1} = 0.02$ (p.u.MW), $\Delta P_{L2} = 0.04$ (p.u.MW), $\Delta P_{L3} = 0.03$ (p.u.MW) at the time $t = 0$ s. Figures 2 to 4 show the change in frequency of areas respectively to three areas. Figures 5 to 7 show the change in tie-line power of the areas.

It can be seen that the frequency deviation of the TSMAPS using the SOISMIC controller, ISMC, and the LQR method is within the allowable range and achieves optimal control efficiency. The difference mainly follows the trend: The PID controller converges to zero. The ISMC and SOISMIC give out a larger spike than PID in areas 1 and 3 (max of PID is at -0.14 Hz in area 2) in the instance load disturbance is introduced. Nevertheless, the SMC controllers oscillate less in three areas, reach the stabilized state, and stay there more stable than PID.

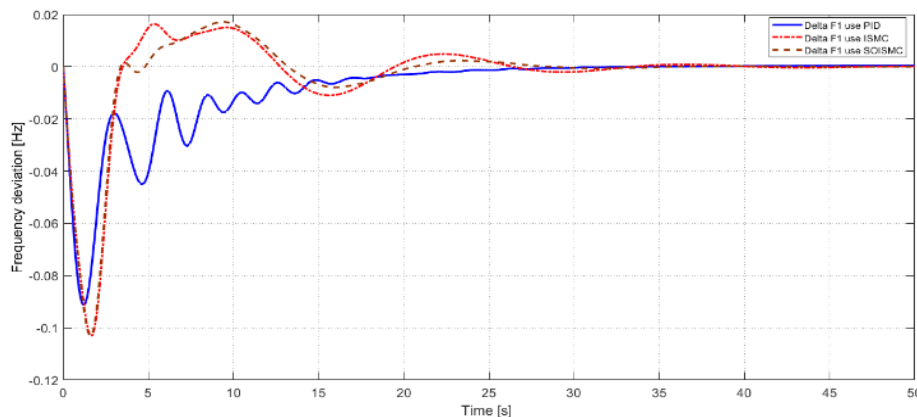


Figure 2. Area 1's frequency deviation using three controllers

The change in tie-line power of three areas gives out interesting features. Despite the robustness and fast reactivity of SMC, PID stabilizes and reaches stability of tie-line faster with fewer oscillations (20 s of PID compared with 40 s of SMCs). The area of highly complex plants (area 3) gives out much more vigorous stabilization of the tie-line, making SMC controllers overshoot and undershoot reaching stability.

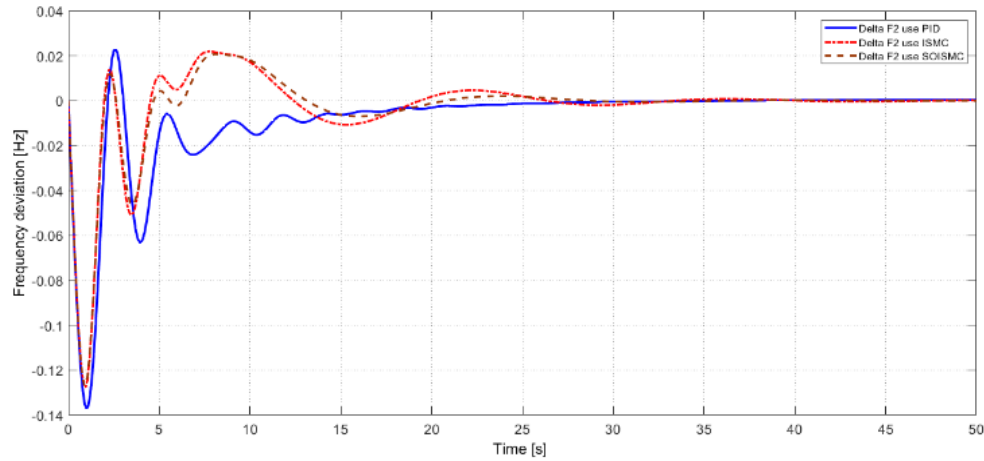


Figure 3. Area 2's frequency deviation using three controllers

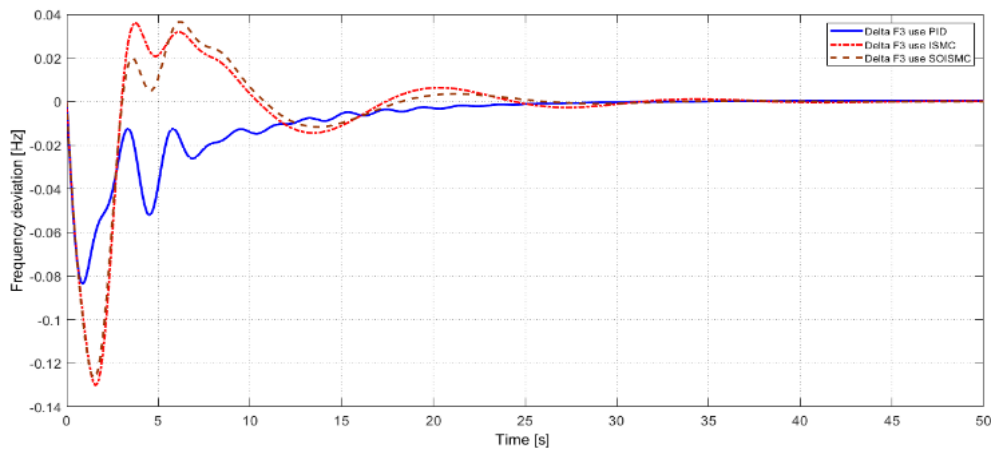


Figure 4. Area 3's frequency deviation using three controllers

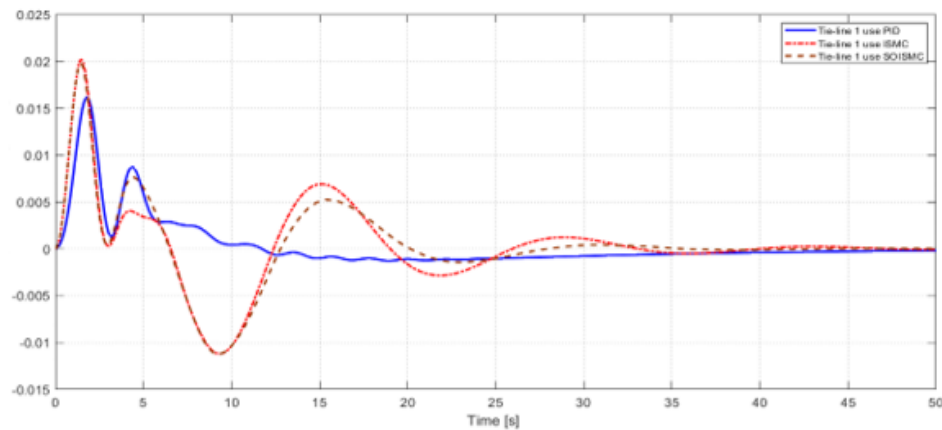


Figure 5. Area 1's tie-line power deviation using three controllers

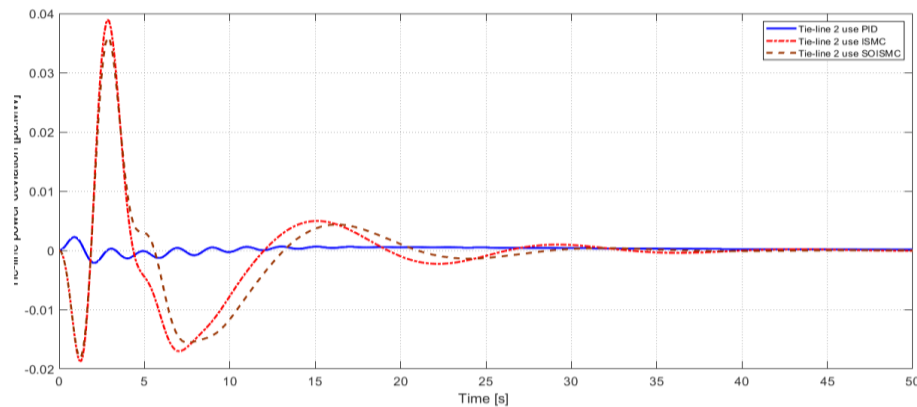


Figure 6. Area 2's tie-line power deviation using three controllers

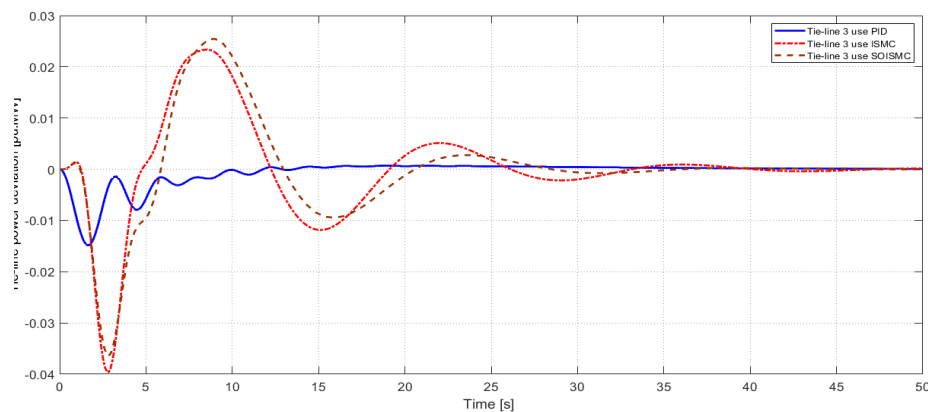


Figure 7. Area 3's tie-line power deviation using three controllers

6. CONCLUSION

This article offers a detailed examination of SMC used for LFC in a combined multi-sources power system. Through thorough simulations and evaluations of performance, numerous important discoveries have highlighted the effectiveness of SOISM. Firstly, SOISM showed better resilience in preserving system frequency stability than traditional control approaches. Furthermore, the SOISM approach successfully integrated hydro and thermal power plants in a single control framework. This combination, along with the simulation shows that the suggested control approach successfully minimizes the frequency variations despite changing load conditions and disturbances, and guarantees that both kinds of power plants can effectively aid in frequency regulation, enhancing the system's overall performance. To sum up, the SOISM technique is shown to be a strong and dependable approach for regulating the behavior of power systems that includes hydro and thermal power plants. This study offers valuable perspectives on improving the stability and efficiency of SMC-based controllers, which will result in more robust and flexible energy management tactics in the future. Possible further work should include implementation of hardware-related SMC-based controllers so as to precisely test and verify the designed controllers.

FUNDING INFORMATION

Authors state no funding involved.

AUTHOR CONTRIBUTIONS STATEMENT

This journal uses the Contributor Roles Taxonomy (CRediT) to recognize individual author contributions, reduce authorship disputes, and facilitate collaboration.

Name of Author	C	M	So	Va	Fo	I	R	D	O	E	Vi	Su	P	Fu
Quoc Thai Phan	✓	✓	✓	✓	✓	✓		✓	✓	✓			✓	
Thinh Lam-The Tran		✓				✓		✓	✓	✓	✓	✓		
Phat Tuan Le	✓		✓	✓			✓			✓	✓		✓	✓
Dinh Bao Ho														
Van Van Huynh					✓		✓			✓		✓		✓

C : Conceptualization

M : Methodology

So : Software

Va : Validation

Fo : Formal analysis

I : Investigation

R : Resources

D : Data Curation

O : Writing - Original Draft

E : Writing - Review & Editing

Vi : Visualization

Su : Supervision

P : Project administration

Fu : Funding acquisition

CONFLICT OF INTEREST STATEMENT

Authors state no conflict of interest.

DATA AVAILABILITY

The authors confirm that the data supporting the findings of this study are available within the article.




REFERENCES

- [1] D. G. Padhan and S. Majhi, "A new control scheme for PID load frequency controller of single-area and multi-area power systems," *ISA Transactions*, vol. 52, no. 2, pp. 242–251, Mar. 2013, doi: 10.1016/j.isatra.2012.10.003.
- [2] R. K. Sahu, S. Panda, and N. K. Yegireddy, "A novel hybrid DEPS optimized fuzzy PI/PID controller for load frequency control of multi-area interconnected power systems," *Journal of Process Control*, vol. 24, no. 10, pp. 1596–1608, Oct. 2014, doi: 10.1016/j.jprocont.2014.08.006.
- [3] V. Veerasamy *et al.*, "Second-order network for decentralized frequency control of multi-microgrid systems," *CSEE Journal of Power and Energy Systems*, pp. 1–12, 2024, doi: 10.17775/CSEEJPES.2023.06510.
- [4] M. Cui, Y. Zhao, P. Cao, Y. Tang, and Y. Lu, "Load frequency control of interconnected hydrothermal power system based on FOPI + FOPD controller," *International Journal of Dynamics and Control*, vol. 12, no. 4, pp. 1073–1085, Apr. 2024, doi: 10.1007/s40435-023-01212-7.
- [5] H. A. Yousef, K. AL-Kharusi, M. H. Albadi, and N. Hosseinzadeh, "Load frequency control of a multi-area power system: an adaptive fuzzy logic approach," *IEEE Transactions on Power Systems*, vol. 29, no. 4, pp. 1822–1830, Jul. 2014, doi: 10.1109/TPWRS.2013.2297432.
- [6] M. Ma, C. Zhang, X. Liu, and H. Chen, "Distributed model predictive load frequency control of the multi-area power system after deregulation," *IEEE Transactions on Industrial Electronics*, vol. 64, no. 6, pp. 5129–5139, Jun. 2017, doi: 10.1109/TIE.2016.2613923.
- [7] L. Dong, Y. Zhang, and Z. Gao, "A robust decentralized load frequency controller for interconnected power systems," *ISA Transactions*, vol. 51, no. 3, pp. 410–419, May 2012, doi: 10.1016/j.isatra.2012.02.004.
- [8] X. Liu, Y. Zhang, and K. Y. Lee, "Coordinated distributed MPC for load frequency control of power system with wind farms," *IEEE Transactions on Industrial Electronics*, vol. 64, no. 6, pp. 5140–5150, Jun. 2017, doi: 10.1109/TIE.2016.2642882.
- [9] W. Wang *et al.*, "Frequency regulation of high-penetration renewable energy microgrids using adaptive model predictive control," *CSEE Journal of Power and Energy System*, 2024, doi: 10.17775/CSEEJPES.2023.04280.
- [10] L. Xiong, H. Li, and J. Wang, "LMI based robust load frequency control for time delayed power system via delay margin estimation," *International Journal of Electrical Power & Energy Systems*, vol. 100, pp. 91–103, Sep. 2018, doi: 10.1016/j.ijepes.2018.02.027.
- [11] S. Wen, X. Yu, Z. Zeng, and J. Wang, "Event-Triggering load frequency control for multiarea power systems with communication delays," *IEEE Transactions on Industrial Electronics*, vol. 63, no. 2, pp. 1308–1317, Feb. 2016, doi: 10.1109/TIE.2015.2399394.
- [12] Y. Shtessel, C. Edwards, L. Fridman, and A. Levant, *Sliding mode control and observation*. New York, NY: Springer New York, 2014.
- [13] V. Van Huynh *et al.*, "New second-order sliding mode control design for load frequency control of a power system," *Energies*, vol. 13, no. 24, p. 6509, Dec. 2020, doi: 10.3390/en13246509.
- [14] K. Liao and Y. Xu, "A robust load frequency control scheme for power systems based on second-order sliding mode and extended disturbance observer," *IEEE Transactions on Industrial Informatics*, vol. 14, no. 7, pp. 3076–3086, Jul. 2018, doi: 10.1109/TII.2017.2771487.
- [15] G. Rinaldi, M. Cucuzzella, and A. Ferrara, "Third order sliding mode observer-based approach for distributed optimal load frequency control," *IEEE Control Systems Letters*, vol. 1, no. 2, pp. 215–220, Oct. 2017, doi: 10.1109/LCSYS.2017.2712564.
- [16] Y. Mi *et al.*, "Sliding mode load frequency control for multi-area time-delay power system with wind power integration," *IET Generation, Transmission & Distribution*, vol. 11, no. 18, pp. 4644–4653, Dec. 2017, doi: 10.1049/iet-gtd.2017.0600.
- [17] S. Prasad, S. Purwar, and N. Kishor, "Non-linear sliding mode control for frequency regulation with variable-speed wind turbine systems," *International Journal of Electrical Power & Energy Systems*, vol. 107, pp. 19–33, May 2019, doi: 10.1016/j.ijepes.2018.11.005.
- [18] A.-T. Tran *et al.*, "Adaptive integral second-order sliding mode control design for load frequency control of large-scale power system with communication delays," *Complexity*, vol. 2021, no. 1, Jan. 2021, doi: 10.1155/2021/5564184.




- [19] Y. Mi *et al.*, "Frequency control strategy of multi-area hybrid power system based on frequency division and sliding mode algorithm," *IET Generation, Transmission & Distribution*, vol. 13, no. 7, pp. 1145–1152, Apr. 2019, doi: 10.1049/iet-gtd.2018.5145.
- [20] A. Kumar, M. N. Anwar, and S. Kumar, "Sliding mode controller design for frequency regulation in an interconnected power system," *Protection and Control of Modern Power Systems*, vol. 6, no. 1, p. 6, Dec. 2021, doi: 10.1186/s41601-021-00183-1.
- [21] J. Guo, "The load frequency control by adaptive high order sliding mode control strategy," *IEEE Access*, vol. 10, pp. 25392–25399, 2022, doi: 10.1109/ACCESS.2022.3152259.
- [22] S. Kuppusamy and Y. H. Joo, "Dynamic integral sliding mode control for interconnected delayed power systems," *Journal of the Franklin Institute*, vol. 359, no. 16, pp. 8742–8757, Nov. 2022, doi: 10.1016/j.jfranklin.2022.08.034.
- [23] J. Ansari, M. Homayounzade, and A. R. Abbasi, "Load frequency control in power systems by a robust backstepping sliding mode controller design," *Energy Reports*, vol. 10, pp. 1287–1298, Nov. 2023, doi: 10.1016/j.egy.2023.08.008.
- [24] H. H. Alhelou, N. Nagpal, N. Kassarwani, and P. Siano, "Decentralized optimized integral sliding mode-based load frequency control for interconnected multi-area power systems," *IEEE Access*, vol. 11, pp. 32296–32307, 2023, doi: 10.1109/ACCESS.2023.3262790.
- [25] S. K. Pradhan and D. K. Das, "Sliding mode controller design via delay-dependent H-inf stabilization criterion for load frequency regulation," *Protection and Control of Modern Power Systems*, vol. 8, no. 1, p. 49, Dec. 2023, doi: 10.1186/s41601-023-00322-w.

BIOGRAPHIES OF AUTHORS






Quoc Thai Phan    was born in Binh Duong province, Vietnam. Currently, he is B.Eng. student in electrical engineering, Ton Duc Thang University, Ho Chi Minh City, Vietnam. His research topics include load frequency control, sliding mode control, and optimal control. He can be contacted at email: 421h0281@student.tdtu.edu.vn.






Thinh Lam-The Tran    was born in Ca Mau City, Vietnam. Currently, he is B.Eng. student in electrical engineering, Ton Duc Thang University, Ho Chi Minh City, Vietnam. His research topics include load frequency control, sliding mode control, and optimal control. He can be contacted at email: 42000133@student.tdtu.edu.vn.






Phat Tuan Le    was born in Dong Nai province, Vietnam. Currently, he is B.Eng. student in electrical engineering, Ton Duc Thang University, Ho Chi Minh City, Vietnam. His research topics include load frequency control, sliding mode control, and optimal control. He can be contacted at email: 421h0289@student.tdtu.edu.vn.



Dinh Bao Ho    was born in Tien Giang province, Vietnam. Currently, he is B.Eng. student in electrical engineering, Ton Duc Thang University, Ho Chi Minh City, Vietnam. His research topics include load frequency control, sliding mode control, and optimal control. He can be contacted at email: 421h0289@student.tdtu.edu.vn.



Van Van Huynh    received the Ph.D. degree in mechanical and automation engineering from Da- Yeh University, Changhua, Taiwan, in 2015. He is currently a Lecturer with the Faculty of Electrical and Electronics Engineering, Ton Duc Thang University, Ho Chi Minh City, Vietnam. His current research interests include sliding mode control, variable structure control, and power system control. He can be contacted at email: huynhvanvan@tdtu.edu.vn.